

This is the accepted manuscript made available via CHORUS. The article has been published as:

Spin-disorder resistivity of ferromagnetic metals from first principles: The disordered-local-moment approach

J. Kudrnovský, V. Drchal, I. Turek, S. Khmelevskiy, J. K. Glasbrenner, and K. D. Belashchenko

Phys. Rev. B **86**, 144423 — Published 31 October 2012

DOI: [10.1103/PhysRevB.86.144423](https://doi.org/10.1103/PhysRevB.86.144423)

Spin-disorder resistivity of ferromagnetic metals from first principles: The disordered-local-moment approach

J. Kudrnovský and V. Drchal

Institute of Physics, Academy of Sciences of the Czech Republic, CZ-182 21 Praha 8, Czech Republic

I. Turek

Charles University, Faculty of Mathematics and Physics,

Department of Condensed Matter Physics, Ke Karlovu 5, CZ-121 16 Praha 2, Czech Republic

S. Khmelevskiy

CMS, Institute of Applied Physics, Vienna University of Technology,

Gußhausstrasse 25a, Makartvilla, 1020, Vienna, Austria

J. K. Glasbrenner and K. D. Belashchenko

*Department of Physics and Astronomy and Nebraska Center for Materials and Nanoscience,
University of Nebraska, Lincoln, Nebraska 68588, USA*

(Dated: October 5, 2012)

The paramagnetic spin-disorder resistivity (SDR) of transition-metal ferromagnets Fe, Co, Ni, ordered transition metal alloys Ni₃Mn and Fe₃Si as well as Ni₂MnX (X=In,Sn,Sb) Heusler alloys is determined from first principles. SDR is evaluated similar to the residual resistivity by using the disordered local moment (DLM) model combined with the Kubo-Greenwood linear response calculation. The electronic structure is determined within the tight-binding linear muffin-tin orbital method and the coherent potential approximation (CPA) applied to the DLM state. We also estimate the temperature dependence of the resistivity below the Curie temperature using a simple model. The results agree well with the supercell Landauer-Büttiker calculations and, generally, with experimental data. For the Ni₂MnSb Heusler alloy it is necessary to include substitutional disorder of B2-type to explain the experimental data.

PACS numbers: 71.23.-k, 72.10.Di, 72.15.-v, 75.50.Bb, 75.50.Cc

I. INTRODUCTION

Temperature dependence of the resistivity is one of the basic properties of a metal. In normal metals and alloys without an external magnetic field, the dominant mechanisms contributing to the resistivity are (i) the residual resistivity due to the scattering of conduction electrons on impurities and other structural defects ρ_{imp} , and (ii) phonon scattering ρ_{ph} . In ferromagnetic metals there is an additional scattering mechanism due to (iii) magnetic fluctuations ρ_{mag} , which usually reach their maximum close to the Curie temperature (T_c).¹⁻³ The latter, spin-disorder part of the resistivity is the subject of this paper. The well-understood resistivity due to phonon scattering⁴ depends linearly on temperature T above the Debye temperature and usually even below it down to fairly low temperatures. The resistivity due to the phonon mechanism has been calculated from first principles for a number of metals, and good agreement with experiment was obtained.⁵ On the other hand, first-principles calculations of the spin-disorder part of the resistivity have not been attempted until recently. Theoretical treatment⁶⁻⁹ based on the s - d model Hamiltonian predicts a quadratic temperature-dependence of the resistivity ρ for low temperatures, a constant, temperature-independent ρ above T_c , and a $\rho \propto [1 - M^2(T)/M_0^2]$ behavior at intermediate temperatures ($M(T)$ and M_0 denote the magnetization at temperatures T and zero, respectively).

The above simple description of the temperature-dependent resistivity is often used in the experiment. The resistivity can be written more generally as

$$\rho(T) = \rho_{imp} + \rho_{ee}(T) + \rho_{ph}(T) + \rho_{mag}(T) + \rho_{mix}(T), \quad (1)$$

where ρ_{imp} , ρ_{ph} , and ρ_{mag} were discussed above. The second term, ρ_{ee} , the contribution due to electron-electron correlations is neglected here as in the most other first-principles studies. In some cases, e.g. in rare-earth metals, the electron correlations are relevant to the electronic structure and modifications are needed. We refer the reader to our recent paper on the subject.¹⁰ Electron correlations are also important in transport studies for low-dimensional systems and at low temperatures (weak localization and conductance fluctuations).¹¹ The last term, ρ_{mix} , contains deviations from the Matthiessen rule, i.e., from the simple sum of above described contributions. For example, it can contain interference terms such as magnon-phonon scattering. Also, the temperature dependence at intermediate

temperatures can be affected by deviations from Matthiessen's rule due to the presence of two spin channels for conduction.¹² The spin-disorder part of the resistivity can also depend on magnetic short-range order, particularly in the critical region around T_c .⁹ We mention that we have also neglected the effect of temperature on the electronic structure which, due to smearing out of the Fermi distribution, may slightly reduce values of local moments and thus the spin-disorder scattering strength. A good agreement between the theory and experiment justifies, at least *a posteriori*, the neglect of ρ_{ee} and ρ_{mix} contributions for systems studied here.

The saturated magnetic resistivity above T_c corresponds to the limit of vanishing spin-spin correlations and it is usually called the spin-disorder resistivity (SDR). It can often be cleanly extracted from experimental measurements taken to sufficiently high temperatures, where the temperature dependence is linear and largely due to phonons. Extrapolation of the phonon contribution to $T = 0$ and subtraction of the residual resistivity gives a reasonable estimate of the experimental value of the SDR to which the theory can be compared.¹³

Quantitative description of the SDR using first-principles calculations requires a consistent averaging procedure. One option is to perform a direct averaging of the Landauer-Büttiker (LB) conductance over spin configurations in supercells; this has been done for Fe and Ni^{16,17} and for heavy rare-earth metals¹⁰. Another option is to use the disordered local moment (DLM) method,¹⁴ which approximates the paramagnetic state as an uncorrelated ensemble of randomly oriented spins and solves the electronic structure problem in the coherent potential approximation (CPA). The Kubo-Greenwood linear response calculation, with proper inclusion of vertex corrections, can then be performed.^{19,20} A semi-empirical approach¹⁸ to calculate the SDR was implemented by assuming a quadratic temperature dependence and calculating the parameters from first principles.

In Ref.15 the SDR was calculated using a hybrid method, in which the electronic structure is described by DLM, and the SDR is calculated in a multilayer geometry as an extrapolation from large values of the imaginary part of energy (1 and 2 mRy) without including vertex corrections. The resulting SDR of Fe and Co was strongly overestimated.

In this paper the SDR is calculated using the DLM method and the standard linear response technique applied in the bulk unit cell with the inclusion of vertex corrections. We consider the transition metals bcc-Fe, fcc-Ni, and fcc-Co, the ordered Ni₃Mn (Cu₃Au structure) and Fe₃Si (D0₃ structure) as well as the Heusler alloys Ni₂MnX, where X=In, Sn, and Sb. The results are compared with experiment and, when available, with first-principles calculations using direct averaging over spin-disordered supercells. Excellent agreement is found between the DLM and supercell methods, as well as with experimental SDR values. The coefficient of the empirical T^2 term for the total resistivity is also calculated for Fe and Ni₂MnSn and is found to agree well with fits to experimental measurements.

II. FORMALISM AND COMPUTATIONAL DETAILS

The electronic structure calculations were performed using the scalar-relativistic tight-binding linear muffin-tin orbital (TB-LMTO) scheme²¹ and the local density approximation (LDA). For the parametrization of the local density functional the Vosko-Wilk-Nusair exchange-correlation potential²³ was used. The effect of disorder (the DLM model) is described by the CPA formulated in the framework of the TB-LMTO Green's function method.²² The same atomic sphere radius was used for all the constituent atoms in the case of ordered and Heusler alloys, and lattice constants were taken from experiment.

In fcc Ni, the DLM moment collapses to zero while the moment in a real material is expected to persist due to longitudinal spin fluctuations.^{24–27} In this case we use the fixed-spin moment (FSM) approach²⁸ and treat the local magnetic moment as an adjustable parameter to recover the experimental value of the SDR, as it was done in Ref.17. Note that this moment is observable and can be measured experimentally using neutron scattering. This approach is also used for Co.

The residual resistivity is determined by the linear-response theory as formulated in the framework of the TB-LMTO-CPA method using the Kubo-Greenwood (KG) formula¹⁹ applied to the DLM state, including vertex corrections.²⁰ (See Appendix A for the justification of the binary alloy analogy for the KG formula.) This approach allows us to include both the substitutional and magnetic disorder on an equal footing, which is necessary for Heusler alloys.

For Fe we also evaluate the SDR using the fully-relativistic (Dirac) version of the KG formula (DKG-DLM) which was implemented recently.²⁹ Some comments are needed, however, concerning the DLM method in the relativistic theory. In the scalar-relativistic case, the spins are decoupled from the lattice, and angular integration for the paramagnetic state can be performed analytically (see Appendix A). In the relativistic case this is no longer true, and the averaging has to be done numerically. In the present case of cubic lattices (bcc, fcc), we have replaced the isotropic spin distribution by a discrete set of 26 directions: six [100] directions along cube edges, twelve [110] directions along face diagonals and eight [111] directions along body diagonals. The weights of these directions were chosen as $c_{[100]} = 1/21 \approx 0.0476$, $c_{[110]} = 4/105 \approx 0.0381$ and $c_{[111]} = 9/280 \approx 0.0321$. With this choice, the averages of the spherical harmonics $Y_{\ell m}(\mathbf{n})$ over the isotropic distribution of unit vectors \mathbf{n} , $\langle Y_{\ell m}(\mathbf{n}) \rangle = \delta_{\ell,0}/\sqrt{4\pi}$, are exactly

reproduced for all $|m| \leq \ell \leq 7$. This approach represents an alternative to the numerical integration over the angles.³⁰ The present choice is restricted to high symmetry directions of the lattice, which guarantees that the local moments are strictly parallel to the local exchange fields, so that no constraining magnetic fields have to be introduced.³¹

To summarize the present approach: the SDR is the resistivity of the completely disordered spin state, which is described by the CPA in the framework of the KG-approach. This is an approximation but is justified by a direct comparison with the more general LB approach. Another problem is the choice of potentials of the randomly disordered spin state used in the KG calculations. The degree of localization and thus the stability of the local magnetic moment increases in the series Ni-Co-Fe-Mn. The conventional DLM potentials are good for rigid moments, i.e. Fe and in particular Mn-based Heusler alloys. If the DLM approach fails like in fcc-Ni, we employ the FSM approach and/or construct the DLM state from potentials of the ferromagnetic state as it was suggested and successfully used in Refs. 10,16,17.

III. RESULTS AND DISCUSSION

In this section we present results for the SDR of transition-metal ferromagnets and selected ordered and Heusler alloys.

A. Transition metal ferromagnets

1. bcc Iron

For bcc Fe we performed KG-DLM calculations with both *spd* and *spdf* basis sets, as well as a fully-relativistic DKG-DLM calculation. The results are summarized in Table I. The magnitude of the local moment in KG-DLM and DKG-DLM is almost the same, and it agrees well with other theoretical calculations and experimental measurements (also listed). The local moment is slightly reduced if the *spdf* basis set is used, as well as in the self-consistent DLM state, in agreement with previous studies.¹⁴ The KG-DLM and DKG-DLM results for SDR agree well with experiment. They also agree well with the LB supercell method of Ref.17; the small difference is mainly due to the small difference in the local moments. In contrast, SDR obtained in the hybrid approach of Ref.15 for the experimental lattice constant is about twice as large.

The effect of vertex corrections in bulk KG calculations (KG-DLM or DKG-DLM) is only a few percent. The main reason for this is the large exchange splitting in Fe. The SDR in DKG-DLM is slightly larger compared to scalar-relativistic KG. A somewhat analogous enhancement was found for some ferromagnetic random alloys, such as Ni-Co or Ni-Fe, where the residual resistivity is appreciably enhanced due to the spin-orbit coupling. In those alloys the relatively large effect stems from the weak disorder in the majority spin channel.⁴¹ In paramagnetic Fe the effect of spin-orbit interaction is weak, because the conduction channels are already strongly mixed by spin disorder.

2. fcc Nickel and Cobalt

In fcc Ni the static local moment in the DLM state is unstable, and the calculation of SDR can not proceed in the usual way. However, electrons are still expected to be scattered by fluctuating local moments.^{24-27,32} In Ref.27 the local moment in fcc Ni near T_c was estimated to be $0.42 \mu_B$. In previous supercell LB calculations¹⁶ the local moment was used as an adjustable parameter, and it was found that agreement with experiment requires the local moment of about $0.35 \mu_B$. Here we follow the same logic without attempting to evaluate the effective local moment in the paramagnetic state. The atomic potentials are prepared using the FSM method by constraining the local moment to several values: 0.6, 0.45, and $0.3 \mu_B$.³⁴ (The self-consistent values in the ferromagnetic state are 0.628 (0.604) μ_B for the *spd* (*spdf*) basis set.)

The results for fcc Ni are summarized in Table II, which also includes the supercell LB results from Ref.17 and the experimental value. The KG-DLM calculations agree well with the LB results for all chosen values of the local moment, including the reduction in the SDR when the *spdf* basis set is used. The experimental SDR is reproduced using a local moment value close to $0.35 \mu_B$ for the *spd*-basis and closer to $0.4 \mu_B$ for the *spdf*-basis.

We have calculated the SDR for fcc Co, which is the stable phase near T_c . (The hcp-phase is stable up to ~ 800 K). There is some controversy regarding the experimental SDR for Co. Two different values were reported: $50 \mu\Omega\text{cm}$ (Ref. 35) and $31 \mu\Omega\text{cm}$ (Ref. 13). The discrepancy is likely due to the insufficient number of data points above T_c ¹³ and the proximity of the melting point $T_m=1768$ K to the Curie temperature $T_c=1400$ K.

The self-consistent local moment of Co in the DLM calculation is $0.964 \mu_B$ for the *spd*-basis and the corresponding SDR is $38.1 \mu\Omega\text{cm}$. The lower experimental value of $31 \mu\Omega\text{cm}$ can be reproduced with a FSM moment of $0.85 \mu_B$; the FSM moment of $1.1 \mu_B$ results in the SDR of $46.2 \mu\Omega\text{cm}$, which is close to the higher experimental estimate of $50 \mu\Omega\text{cm}$. As for Ni, the SDR calculated using the *spdf* basis set are somewhat smaller. For example, for the FSM local moment of $0.9 \mu_B$ the SDR is 34.3 (30.1) $\mu\Omega\text{cm}$ for the *spd* (*spdf*) basis set, respectively. Note that the value of SDR obtained in the hybrid approach of Ref.15 is $100\text{--}180 \mu\Omega\text{cm}$ depending on the value of the lattice constant.

B. Ordered metallic alloys Ni_3Mn and Fe_3Si

In this section we calculate the SDR for more complicated alloys, including Cu_3Au -ordered Ni_3Mn and D0_3 -ordered Fe_3Si . It should be mentioned that e.g. Fe_3Si exhibits a complex pressure-dependent metamagnetic behavior.³⁶ Here we limit ourselves to ambient pressure where studied systems are conventional ferromagnets.

The Cu_3Au lattice is formed by four interpenetrating simple cubic sublattices occupied by Ni and Mn atoms; the three Ni sublattices are equivalent. The experimental SDR value of $72 \mu\Omega\text{cm}$ was extracted from Fig. 7 of Ref. 1 by subtracting the phonon part. The experiment also shows a non-zero residual resistivity (about $20 \mu\Omega\text{cm}$) which may be due to chemical disorder or off-stoichiometry. As in pure fcc Ni, the local moments on Ni atoms collapse to zero in the DLM state. We made two calculations, one based on the self-consistent DLM potentials (*spd* basis) with spin disorder limited to Mn atoms (their local moment is $3.179 \mu_B$), and another one with the DLM potentials constructed from the collinear ferromagnetic ground state¹⁷ (the local moments on Ni (Mn) sites are 0.467 (3.183) μ_B). The local moment of Mn is rigid and essentially independent on the magnetic state. The calculated SDR values for the two calculations are, respectively, $23.6 \mu\Omega\text{cm}$ and $58.9 \mu\Omega\text{cm}$. The latter value, which accounts for the additional spin disorder on Ni atoms, agrees reasonably well with experiment, considering the fact that we assumed ideal stoichiometry.

As mentioned above, in some Ni-based alloys, such as fcc NiCo and NiFe , the spin-orbit coupling has a pronounced effect on the resistivity due to the mixing of the weakly-disordered majority and strongly-disordered minority-spin channels, which gives rise to an additional contribution to the resistivity.²⁹ The situation in the DLM state of Ni_3Mn is different, because both channels are disordered. We have calculated the SDR using DLM potentials constructed from the ferromagnetic state and including the spin-orbit coupling perturbatively.²⁹ The resulting SDR of $62.0 \mu\Omega\text{cm}$ is only slightly larger compared to the scalar-relativistic case ($58.9 \mu\Omega\text{cm}$). These results suggest that the Ni atoms in Ni_3Mn retain effective local moments above T_c as in the known case of fcc Ni (see Section III A 2).

The calculations for D0_3 -ordered Fe_3Si were also performed using the *spd* basis. Due to symmetry, there are two inequivalent Fe sites in this alloy. The sites (Fe_1) surrounded by eight Fe atoms have a large and robust local moment of $2.555 \mu_B$, while sites (Fe_2) surrounded by four Fe and four Si atoms have a significantly reduced moment of $1.320 \mu_B$. There is also a small local moment on the Si sites ($-0.095 \mu_B$). In the DLM state, the Fe_1 local moments remain essentially the same ($2.719 \mu_B$), but the Fe_2 local moments collapse to zero. The Si local moments are also zero in the DLM state. As above for Ni_3Mn , we performed two calculations, one based on self-consistent potentials in the DLM state with spin disorder only on Fe_1 sites, and another one with the DLM potentials taken from the ferromagnetic ground state. The resulting SDR values are $146.7 \mu\Omega\text{cm}$ and $181.9 \mu\Omega\text{cm}$, respectively. These results compare well with the experimental value of about $170 \mu\Omega\text{cm}$.³⁷

C. Heusler alloys Ni_2MnX , $\text{X}=\text{In, Sn, Sb}$

Heusler alloys is another group of magnetic metals with a complex lattice structure for which experimental data are available in the literature. These alloys have L2_1 -structure formed by four interpenetrating fcc sublattices mutually shifted along the body-diagonal with the sublattice occupation Ni-Mn-Ni-X. We employ the *spdf* basis and the DLM model for the Mn sublattice. Small induced magnetic moments on the Ni and Sb atoms in the ferromagnetic state collapse in the DLM state, and their effect is neglected. The number of the valence electrons increases in the series from In to Sn to Sb.

The calculated KG-DLM SDR are summarized in Table III together with the experimental data. The SDR for Ni_2MnSn was also calculated using the supercell LB approach.¹⁷ (See Appendix B for details.) The KG-DLM and LB calculations for Ni_2MnSn agree again very well.⁴⁴

There is good agreement with experiment for Ni_2MnSn (see also Ref. 18) and Ni_2MnIn , but not for Ni_2MnSb , where the calculated SDR is more than twice larger. The origin of this discrepancy in Ni_2MnSb can be traced back to the fact that the structure of some Heusler alloys depends sensitively on the sample preparation and annealing. This can be clearly seen from the residual resistivities at $T=0$ K, which are negligible for Ni_2MnSn and Ni_2MnIn and rather large ($65\text{--}68 \mu\Omega\text{cm}$) for Ni_2MnSb .^{38,39}

We have considered Mn-Sb swapping (B2 disorder) as a likely source of the residual resistivity, which is typical for some Heusler alloys like e.g. Ni_2MnAl alloy.⁴⁵ Corresponding theoretical calculations favor the antiparallel orientation of Mn[Mn] and Mn[Al] moments.⁴⁶ Possible short-range effects due to a chemical disorder are neglected here due to the use of the CPA. These effects can be included, however, in the framework of the LB approach. It is not anticipated that short-range interactions would have a noticeable effect on the electronic band structure of the Heusler alloys.⁴⁸ The present total energy calculations also confirm the antiparallel orientations of Mn[Sb] moments with respect to Mn[Mn] moments (ferrimagnetic state). As before, only Mn atoms were treated within the DLM method, but now on both Mn and Sb sublattices. The difference between the resistivities in the DLM and the ground state (with antiparallel alignment of Mn local moments on the “wrong” sublattice) corresponds to the measured SDR. From the data of Ref.38 and the fact that the Curie temperature ranges from 344 K³⁸ to 360 K,³⁹ we estimated the SDR as 30.5-36 $\mu\Omega\text{cm}$. This value can be compared with the calculated values of 55.1 $\mu\Omega\text{cm}$ and 44.0 $\mu\Omega\text{cm}$ for 15% and 20% Mn-Sb swapping, respectively. Thus, the Mn-Sb swapping strongly reduces the calculated SDR. As a result, there is a fair agreement between theory and experiment considering the uncertainties of the accurate extraction of the SDR from measured T -dependent resistivities and of the assumptions about the source of the residual resistivity.

D. Remark on the resistivity of bcc-Fe below T_c

The theoretical determination of the T -dependent resistivity is a difficult problem. One approach to this problem is to construct supercells and average the conductance over the real-space spin configurations modeled either by a mean-field distribution or by Monte-Carlo simulations for the classical Heisenberg model. Although the latter approach includes a number of approximations, it is particularly suitable for including magnetic short-range order (MSRO) effects.¹⁷

A simpler approach can be used for systems with weak MSRO, such as bcc Fe¹⁷ or some Heusler alloys.¹⁸ As mentioned in the Introduction, for very low and intermediate temperatures the resistivity varies with temperature as $\rho \propto T^2$ and $\rho \propto [1 - M^2(T)/M_0^2]$, respectively. The temperature dependence of the total resistivity appears to be well approximated by $\rho(T) = \rho_o + AT + CT^2$ in some Heusler alloys.³⁸ Here ρ_o is the residual resistivity, the linear term A is extracted from the high-temperature region of the resistivity and subtracted (together with ρ_o) from the total resistivity. The remaining magnetic contribution can then be fitted to CT^2 .

It should be emphasized that such dependence represents only an empirical observation for some ferromagnets. From the theoretical point of view, it is interesting that in such cases the coefficient $C = \rho(T_c)/T_c^2$. If one identifies $\rho(T_c)$ with $\rho(\text{DLM})$ evaluated in the KG-DLM or DKG-DLM approaches, and T_c is also determined from first principles, one can estimate the T -dependence of resistivity and compare it with experiment. Such a program was successfully tested for Ni_2MnSn and Pd_2MnSn Heusler alloys,¹⁸ and here we apply it to bcc Fe.

Using the *spdf* basis and the DLM state as a reference for constructing the Heisenberg Hamiltonian, we obtained $T_c = 1105$ K in the random-phase approximation (see Ref. 47 for computational details.) The experimental value is 1040 K. The calculated SDR is 71.5 (75.2) $\mu\Omega\text{cm}$ for KG-DLM (DKG-DLM), respectively. We thus estimate $C=0.586$ (0.616) $\times 10^{-4}$ $\mu\Omega\text{cm}/\text{K}^2$.

To compare with experiment, we used the electrical resistivity data for Fe from Ref. 13 and subtracted the phonon part as indicated above (the experimental residual resistivity is very small). The result is $C = 0.647 \times 10^{-4}$ $\mu\Omega\text{cm}/\text{K}^2$ in fair agreement with the KG-DLM and DKG-DLM calculations.

IV. CONCLUSIONS

We have presented a simple theory of paramagnetic spin-disorder resistivity based on the disordered local moment model combined with the Kubo-Greenwood linear-response technique and applied it to magnetic transition metals, ordered Ni_3Mn and Fe_3Si compounds, and to Ni_2MnX ($X=\text{In, Sn, Sb}$) Heusler alloys. The results agree reasonably well with experimental data and with the results of the supercell Landauer-Büttiker approach (bcc Fe, fcc Ni, and Ni_2MnSn). The case of Ni (and partly also Co) requires a special approach in which the FSM-DLM method is used. Present results, in an agreement with a recent study¹⁷ indicate an interesting relation between the local moments in the magnetically disordered state and the SDR, in particular in cases where the local moment is induced by the longitudinal spin fluctuations (such as fcc Ni).²⁷

We have also calculated the SDR for ordered Ni_3Mn and Fe_3Si alloys. The local moments on Ni in Ni_3Mn and on one of the Fe sublattices in Fe_3Si collapse to zero in the DLM state, but in reality these moments may persist due to quantum and thermal fluctuations. In order to evaluate their effect on SDR, we used two models with potentials taken either from the DLM state or from the ferromagnetic state. For Ni_3Mn our results suggest that Ni atoms retain

their local moments above T_c . In Fe_3Si the SDR in both models is close to experiment, so that a clear conclusion can not be drawn.

The SDR value in Ni_2MnSb can be explained only by assuming the presence of disorder in an otherwise stoichiometric alloy. Other studied Heusler alloys exhibit only very small residual resistivity, and the KG-DLM model applied to ideal systems works well. Finally, we have shown that a reasonable description of the resistivity below T_c is possible for metals with a weak magnetic short-range order like, e.g., bcc-Fe¹⁷ or some Heusler alloys.¹⁸ We conclude that the linear response calculation of the spin-disorder resistivity within the DLM model is a rather fast and accurate alternative to the computationally demanding averaging of the Landauer-Büttiker conductance over spin-disorder configurations in supercells. This method is applicable as long as uncorrelated spin disorder is being considered.

Acknowledgments

J.K., V.D., and I.T. acknowledge support of the Czech Science Foundation (Grant No. P204/11/1228). The work at UNL was supported by the NSF through Grant No. DMR-1005642 and Nebraska MRSEC (Grant No. DMR-0820521). K.D.B. acknowledges financial support from the Research Corporation through the Cottrell Scholar Award. S.Kh. acknowledges the Austrian FWF (SFB ViCoM F4109-N13) for financial support.

Appendix A: Alloy analogy for conductivity of the DLM state

The residual conductivity of a random alloy reduces within the TB-LMTO-CPA formalism to expressions of the form

$$\begin{aligned} \text{Tr} \langle g(z) v g(z') v \rangle &= \text{Tr} \{ \bar{g}(z) v \bar{g}(z') v \} \\ &+ \text{Tr} \{ \bar{g}(z) \Gamma(z, z') \bar{g}(z') v \}, \end{aligned} \quad (\text{A1})$$

where the symbol $\langle \dots \rangle$ denotes configuration averaging, the $g(z)$ is the auxiliary Green's function, the v denotes a non-random effective velocity operator, and the energy arguments $z, z' = E_F \pm i0$, where the E_F is the alloy Fermi energy.¹⁹ The first term in Eq. (A1) leads to the coherent contribution to the conductivity, with $\bar{g}(z) = \langle g(z) \rangle$, while the second term represents the incoherent (vertex) contribution. The non-random quantity $\Gamma(z, z')$ is given as a sum over lattice sites, $\Gamma(z, z') = \sum_{\mathbf{R}} \Gamma_{\mathbf{R}}(z, z')$, where the individual terms can be obtained from a set of coupled linear equations

$$\begin{aligned} \Gamma_{\mathbf{R}}(z, z') &= \langle t_{\mathbf{R}}(z) \bar{g}(z) v \bar{g}(z') t_{\mathbf{R}}(z') \rangle \\ &+ \sum_{\mathbf{R}' (\neq \mathbf{R})} \langle t_{\mathbf{R}}(z) \bar{g}(z) \Gamma_{\mathbf{R}'}(z, z') \bar{g}(z') t_{\mathbf{R}}(z') \rangle, \end{aligned} \quad (\text{A2})$$

where the $t_{\mathbf{R}}(z)$ denotes the random single-site T-matrix operator at the \mathbf{R} -th site defined with respect to the effective CPA medium, see Ref. 20 for details. The solution of these equations can be obtained as a limit for $n \rightarrow \infty$ of the sequence $\Gamma_{\mathbf{R}}^{(n)}(z, z')$, $n = 1, 2, \dots$, which is defined recursively by

$$\begin{aligned} \Gamma_{\mathbf{R}}^{(1)} &= \langle t_{\mathbf{R}} \bar{g} v \bar{g} t_{\mathbf{R}} \rangle, \\ \Gamma_{\mathbf{R}}^{(n+1)} &= \Gamma_{\mathbf{R}}^{(1)} + \sum_{\mathbf{R}' (\neq \mathbf{R})} \langle t_{\mathbf{R}} \bar{g} \Gamma_{\mathbf{R}'}^{(n)} \bar{g} t_{\mathbf{R}} \rangle, \end{aligned} \quad (\text{A3})$$

with energy arguments z and z' omitted here and below for brevity.

The application of this approach to the DLM state with local magnetic moments pointing randomly in all directions leads to the average Green's function $\bar{g}(z)$ that is spin-independent. In each spin channel, the \bar{g} is defined from an equiconcentration random alloy of two atomic species, corresponding to moments pointing up and down which lead to single-site T-matrices $t_{\mathbf{R}}^{\uparrow}$ and $t_{\mathbf{R}}^{\downarrow}$ satisfying the CPA condition $t_{\mathbf{R}}^{\uparrow} + t_{\mathbf{R}}^{\downarrow} = 0$.¹⁴ For conductivity calculations, the effective velocity operator is given by the commutator relation $v = -i[X, S]$, where the X represents the coordinate operator and the S denotes the TB-LMTO structure-constant matrix.¹⁹ Consequently, the v is spin-independent as well and the coherent part of the DLM conductivity can thus be evaluated very easily in the alloy analogy.¹⁴

For the vertex part of the conductivity, one can write the spin-independent operators (matrices) \bar{g} , v and $\bar{g}v\bar{g}$ in Eq. (A3) in the form

$$M = m \otimes 1, \quad (\text{A4})$$

where the first factor denotes a matrix in the site- and orbital-index $\mathbf{R}L$ ($L = \ell m$) while the second factor is the unit matrix in the spin index s ($s = \uparrow, \downarrow$). In this notation, the single-site T-matrix for the \mathbf{R} -th local moment pointing in a random direction $\mathbf{n}_{\mathbf{R}}$ can be written as

$$t_{\mathbf{R}} = \frac{t_{\mathbf{R}}^{\uparrow} + t_{\mathbf{R}}^{\downarrow}}{2} \otimes 1 + \frac{t_{\mathbf{R}}^{\uparrow} - t_{\mathbf{R}}^{\downarrow}}{2} \otimes \sum_{\alpha} n_{\mathbf{R}\alpha} \sigma_{\alpha}, \quad (\text{A5})$$

where $\alpha = x, y, z$, the $n_{\mathbf{R}\alpha}$ are components of the random unit vector $\mathbf{n}_{\mathbf{R}}$ and the σ_{α} denote the Pauli spin matrices. By using the identity $\sigma_{\alpha}^2 = 1$ and the obvious configuration averages $\langle n_{\mathbf{R}\alpha} \rangle = 0$ and $\langle n_{\mathbf{R}\alpha} n_{\mathbf{R}\beta} \rangle = \delta_{\alpha\beta}/3$, one can prove easily that for an arbitrary non-random spin-independent operator M , Eq. (A4), the following averaging rule is valid:

$$\begin{aligned} \langle t_{\mathbf{R}} M t_{\mathbf{R}} \rangle &= \mu \otimes 1, \\ \mu &= \frac{1}{2} t_{\mathbf{R}}^{\uparrow} m t_{\mathbf{R}}^{\uparrow} + \frac{1}{2} t_{\mathbf{R}}^{\downarrow} m t_{\mathbf{R}}^{\downarrow}. \end{aligned} \quad (\text{A6})$$

This means that the resulting average $\langle t_{\mathbf{R}} M t_{\mathbf{R}} \rangle$ is spin-independent and that it can be obtained again by employing the equiconcentration alloy of up- and down-moments. The use of Eq. (A6) in the recursive sequence (A3), i.e., for $M = \bar{g}v\bar{g}$ and $M = \bar{g}\Gamma_{\mathbf{R}}^{(n)}\bar{g}$, $n = 1, 2, \dots$, proves that the alloy analogy is applicable also for evaluation of the vertex part of the DLM conductivity.

Appendix B: Landauer-Büttiker calculation for Ni_2MnSn

The Landauer-Büttiker supercell method used as a benchmark to calculate the SDR of the Heusler alloy Ni_2MnSn was described in Ref. 17. The *spd* basis set and the Barth-Hedin exchange-correlation potential⁴² were used to solve the electronic structure problem and for transport calculations. The ground-state local moments and total density of states agree well with previously reported data.^{18,43} For the transport calculations, a 2×2 lateral cubic supercell was used. Good convergence was achieved by integrating the conductance over the two-dimensional Brillouin zone using a 15×15 k -point mesh and averaging over 15 random noncollinear spin distributions (spin disorder applied to Mn moments only). The active disordered region was varied in length from 4 monolayers to 104 monolayers, as shown in Fig. 1, reaching the Ohmic regime. The calculated SDR for Ni_2MnSn was $47.7 \pm 0.4 \mu\Omega \text{ cm}$, which is in excellent agreement with the DLM method and with experiment.

-
- ¹ B. R. Coles, Adv. Phys. **7**, 40 (1958).
 - ² N. F. Mott, Adv. Phys. **13**, 325 (1964).
 - ³ S. V. Vonsovskii, Magnetism (Halsted, New York, 1974).
 - ⁴ J.M. Ziman, *Electrons and Phonons*, Oxford (1960).
 - ⁵ E. G. Maksimov, D. Yu. Savrasov, and S. Yu. Savrasov, Sov. Phys.-Usp. **40**, 337 (1997).
 - ⁶ T. Kasuya, Prog. Theor. Phys. **16**, 58 (1956).
 - ⁷ T. Kasuya, Prog. Theor. Phys. **22**, 227 (1959).
 - ⁸ P.G. de Gennes and J. Friedel, J. Phys. Chem. Solids **4**, 71 (1958).
 - ⁹ M.E. Fisher and J.S. Langer, Phys. Rev. Lett. **20**, 665 (1968).
 - ¹⁰ J.K. Glasbrenner, K.D. Belashchenko, J. Kudrnovský, V. Drchal, S. Khmelevskyi, and I. Turek, Phys. Rev. B **85**, 214405 (2012).
 - ¹¹ P.A. Lee and T.V. Ramakrishnan, Rev. Mod. Phys. **57**, 287 (1985).
 - ¹² A. Fert and I. A. Campbell, Phys. Rev. Lett. **21**, 1190 (1968); J. Phys. F: Met. Phys. **6**, 849 (1976).
 - ¹³ J. Bass and K.H. Fischer in *Landolt-Börnstein* New Series Group III, Vol. 15a, K.-H. Hellwege and J.L. Olsen (Eds.) (Springer, Berlin, 1982) p. 1.
 - ¹⁴ B.L. Gyorffy, A.J. Pindor, J. Staunton, G.M. Stocks, and H. Winter, J. Phys. F: Metal Phys. **15**, 1337 (1985).
 - ¹⁵ A. Burusz, L. Szunyogh, and P. Weinberger, Philos. Mag. **88**, 2615 (2008).
 - ¹⁶ A. Wysocki, K.D. Belashchenko, and J.P. Velez, J. Appl. Phys. **101**, 09G506 (2007).
 - ¹⁷ A. Wysocki, R.F. Sabirianov, M. van Schilfgaarde, and K.D. Belashchenko, Phys. Rev. B **80**, 224423 (2008).
 - ¹⁸ S.K. Bose, J. Kudrnovský, V. Drchal, and I. Turek, Phys. Rev. B **82**, 174402 (2010).
 - ¹⁹ I. Turek, J. Kudrnovský, V. Drchal, L. Szunyogh, and P. Weinberger, Phys. Rev. B **65**, 125101 (2002).
 - ²⁰ K. Carva, I. Turek, J. Kudrnovský, and O. Bengone, Phys. Rev. B **73**, 144421 (2006).
 - ²¹ O.K. Andersen and O. Jepsen, Phys. Rev. Lett. **53**, 2571 (1984).

- ²² I. Turek, V. Drchal, J. Kudrnovský, M. Šob, and P. Weinberger, *Electronic Structure of Disordered Alloys, Surfaces and Interfaces* (Kluwer, Boston, 1997); I. Turek, J. Kudrnovský and V. Drchal, in *Electronic Structure and Physical Properties of Solids*, edited by H. Dreyssé, Lecture Notes in Physics, Vol. **535** (Springer, Berlin, 2000), p. 349.
- ²³ S.H. Vosko, L. Wilk, and M. Nusair, Can. J. Phys. **58**, 1200 (1980).
- ²⁴ T. Moriya, Spin Fluctuations in Itinerant Electron Magnetism (Springer, Berlin, 1985).
- ²⁵ M. Uhl and J. Kübler, Phys. Rev. Lett. **77**, 334 (1996).
- ²⁶ N. M. Rosengaard and B. Johansson, Phys. Rev. B **55**, 14975 (1997).
- ²⁷ A.V. Ruban, S.K. Khmelevskyi, P. Mohn, and B. Johansson, Phys. Rev. B **75**, 054402 (2007).
- ²⁸ V.L. Moruzzi, P.M. Marcus, K. Schwarz, and P. Mohn, Phys. Rev. B **34**, 1784 (1986).
- ²⁹ I. Turek, J. Kudrnovský, and V. Drchal, Phys. Rev. B **86**, 014405 (2012).
- ³⁰ J.B. Staunton, L. Szunyogh, A. Buruzs, B.L. Gyorffy, S. Ostanin, and L. Udvardi, Phys. Rev. B **74**, 144411 (2006).
- ³¹ B. Ujfalussy, X.D. Wang, D.M.C. Nicholson, W.A. Shelton, G.M. Stocks, Y. Wang, and B.L. Gyorffy, J. Appl. Phys. **85**, 4824 (1999).
- ³² A. L. Wysocki, J. K. Glasbrenner, and K. D. Belashchenko, Phys. Rev. B **78**, 184419 (2008).
- ³³ M. Acet, E.F. Wassermann, K. Andersen, A. Murani, and O. Schärff, Europhys. Lett. **40**, 93 (1997).
- ³⁴ To check the consistency of the FSM method, we have compared the SDR for fcc Co calculated using the atomic potentials taken from the paramagnetic DLM calculation and those taken from the FSM state constraining the local moments to the same values. The calculated SDR were identical.
- ³⁵ R.J. Weiss and A.S. Marotta, J. Phys. Chem. Solids **9**, 302 (1959).
- ³⁶ J.Y. Rhee and B.N. Harmon, Phys. Rev. B **70**, 094411 (2004).
- ³⁷ Y. Nishino, S. Innoue, and S. Asano, Phys. Rev. B **48**, 13607 (1993).
- ³⁸ W.H. Schreiner, D.E. Brandao, F. Ogiba, and J.V. Kunzler, J. Phys. Chem. Solids **43**, 777 (1982).
- ³⁹ C.M. Hurd and S.P. McAlister, J. Mag. Mag. Mater. **61**, 114 (1986).
- ⁴⁰ G. Grimvall, Phys. Rev. B **39**, 12300 (1989).
- ⁴¹ J. Banhart, H. Ebert and A. Vernes, Phys. Rev. B **56**, 10165 (1997).
- ⁴² U. von Barth and L. Hedin, J. Phys. C: Solid State Phys. **5**, 1629 (1972).
- ⁴³ Y. Kurtulus, R. Dronskowski, G. D. Samolyuk, and V. P. Antropov, Phys. Rev. B **71**, 014425 (2005).
- ⁴⁴ Note some technical differences between KG-DLM and sc-LB approaches: DLM state, *spdf*-basis, Vosko-Wilk-Nusair local exchange (KG-DLM) and DLM potentials constructed from the ferromagnetic state, *spd*-basis, and von Barth-Hedin local exchange (sc LB). The SDR in the KG-DLM for DLM state and *spd*-basis is very similar, namely 51.0 $\mu\Omega\text{cm}$.
- ⁴⁵ M. Acet, E. Duman, E.F. Wassermann, L. Manosa, and A. Planes, J. Appl. Phys. **92**, 3867 (2002).
- ⁴⁶ I. Galanakis and E. Şaşıoğlu, Appl. Phys. Lett. **98**, 102514 (2011).
- ⁴⁷ I. Turek, J. Kudrnovský, V. Drchal, and P. Bruno, Philos. Mag. **86**, 1713 (2006).
- ⁴⁸ K. Özdoğan, E. Şaşıoğlu, and I. Galanakis, J. Appl. Phys. **103**, 023503 (2008).

TABLE I: Calculated SDR (ρ_{SDR}) for bcc-Fe in the present approach (KG-DLM) and in the supercell LB (sc-LB)^{16,17} are compared with its experimental value (ρ_{exp}).¹³ The value of the SDR from the Landauer-DLM approach¹⁵ is 180 $\mu\Omega\text{cm}$. Present results obtained using the fully relativistic (Dirac) version of the KG-DLM approach (DKG-DLM²⁹) are also shown. We present the magnetic moments in the ferromagnetic phase ($M_{\text{tot}}^{\text{FM}}$) and in the DLM phase ($M_{\text{tot}}^{\text{DLM}}$) when available. Results are shown for the *spd*-basis while corresponding values for *spdf*-basis are given in brackets. The experimental lattice constant of bcc-Fe was used.

	Method			
	KG-DLM	DKG-DLM	sc-LB	exper
$M_{\text{tot}}^{\text{FM}} (\mu_B)$	2.23 (2.18)	2.23 (2.19)	2.29 (2.22)	2.18
$M_{\text{tot}}^{\text{DLM}} (\mu_B)$	2.15 (2.06)	2.18 (2.08)	—	—
$\rho_{\text{SDR}} (\mu\Omega\text{cm})$	84.7 (71.5)	89.6 (75.2)	102 (85)	80

TABLE II: The calculated SDR (ρ_{SDR}) for ferromagnetic fcc-Ni in the present KG-DLM approach are compared with the results of the supercell LB (sc-LB) approach.^{16,17} The experimental value is 15 $\mu\Omega\text{cm}$.^{13,35} Calculated resistivities are presented as a function of the effective Ni-local moment M_{eff} . Results are shown for the *spd*-basis while corresponding values for *spdf*-basis are given in brackets. In the case of the sc-LB approach we also show theoretical errorbars (see text for details).¹⁷ The experimental lattice constant of fcc-Ni was used.

Method	$M_{\text{eff}} (\mu_B)$	$\rho_{\text{SDR}} (\mu\Omega\text{cm})$
KG-DLM	0.3	12.4 (10.2)
	0.45	26.7 (19.7)
	0.6	34.1 (29.7)
sc-LB	0.3	12 \pm 0.3
	0.4	21 \pm 0.4 (18 \pm 0.4)
	0.5	27 \pm 0.5 (23 \pm 0.5)
	0.66	34 \pm 0.6 (29 \pm 0.6)

TABLE III: Calculated theoretical SDR (ρ_{th}) in Heusler alloys Ni_2MnX ($X=\text{In, Sn, Sb}$) in the KG-DLM approach are compared with corresponding experimental data (ρ_{exp}).^{38,39} The DLM is limited to the Mn-sublattice. For all alloys the experimental lattice constants was used. See the text for discrepancy between theory and experiment for Ni_2MnSb alloy.

Alloy	$\rho_{\text{th}} (\mu\Omega\text{cm})$	$\rho_{\text{exp}} (\mu\Omega\text{cm})$
Ni_2MnIn	42.6	44.1
Ni_2MnSn	50.4	46.6
Ni_2MnSb	73.7	31–35

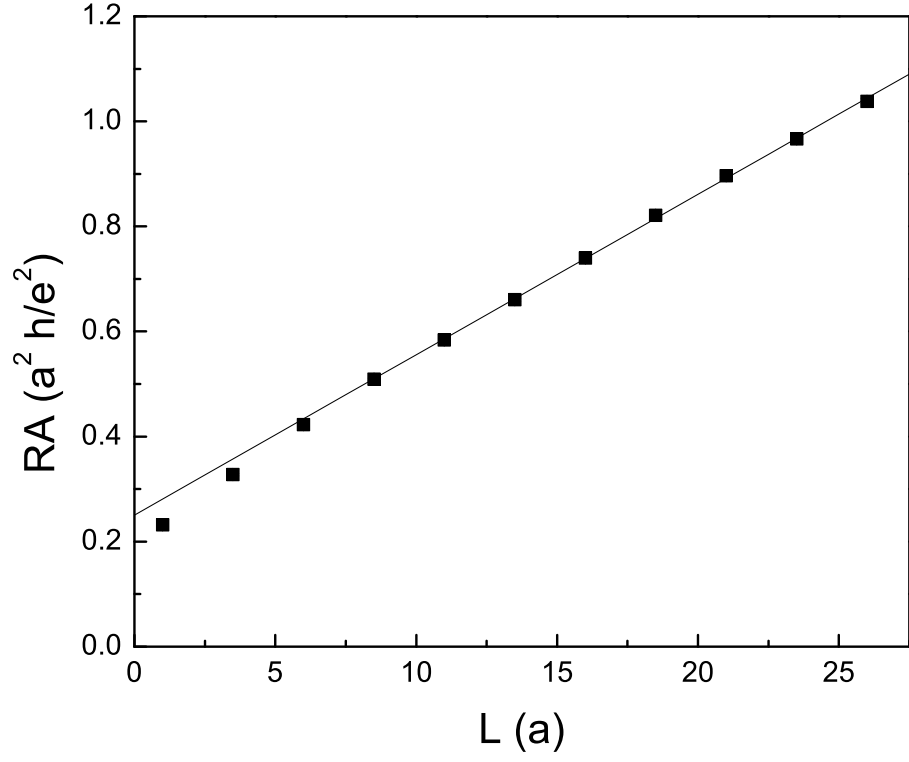


FIG. 1: Area-resistance product RA *vs* the thickness L (4 monolayers per lattice constant a) of the disordered region for Ni_2MnSn . Each point corresponds to an average of 15 random spin-disorder configurations.